

## Lattice-Site Determination by Magnetic Hyperfine Interaction for Implanted $^{54}\text{Fe}$ Ions in $\alpha$ - and $\gamma$ -Cerium

S. Seeger, H. H. Bertschat, K. H. Biedermann, J. P. Biersack, H. Haas, R. Kowallik, H.-E. Mahnke,  
W. Müller, and W.-D. Zeitz

*Bereich Schwerionenphysik, Hahn-Meitner-Institut Berlin GmbH, Postfach 390128, D-1000 Berlin 39, Germany*

(Received 27 December 1989)

A pronounced difference in magnetic behavior at distinct lattice sites has been found for recoil-implanted  $^{54}\text{Fe}$  ions in fcc cerium metal using the perturbed-angular-distribution method. Of the implanted ions 25(5)% show predominantly spin magnetism while 75(5)% appear to be nonmagnetic. Based on the Anderson model, the magnetic fraction is assigned to regular lattice sites and the nonmagnetic fraction is inferred to occupy interstitial positions. This interpretation is supported by Monte Carlo simulations describing the transport of ions in matter.

PACS numbers: 76.30.Fc, 61.80.Jh, 75.20.Hr, 75.30.Hx

With the increasing numbers of experimental studies in radiation effects, in ion-beam modification of solids, and especially in ion-implantation techniques, the determination of the final site of implanted ions in host materials gains importance for any detailed understanding. The creation of damage and related effects is investigated by standard methods, such as resistivity measurements or electron and x-ray diffraction. However, the determination of the final lattice site of the implanted ion requires the application of microscopic methods which are sensitive to local environments on an atomic scale, such as channeling, Mössbauer spectroscopy, low-temperature nuclear orientation, or the perturbed-angular-correlation (PAC) and -distribution (PAD) methods.

The PAD method in particular combines ion implantation and the investigation of ion location on a microscopic scale simultaneously. Ions are produced by nuclear reactions and implanted by their recoil energy into any host. Hyperfine interactions of the nuclear moments in the lattice sensitively depend on the electric-field gradients and/or magnetic fields of the local environment. One advantage of this method is that it is applicable for a large variety of elements since many probe nuclei with suitable nuclear properties are known.<sup>1</sup>

Theoretical predictions concerning the final site of implanted ions are scarce and suffer from major uncertainties. Several approaches have been proposed. Within the Hume-Rothery rules, particularly the metallurgical aspects of the system are considered.<sup>2</sup> Miedema and Niessen<sup>3</sup> propose a binary-alloy model on the basis of ordering phenomena. Brice<sup>4</sup> considers the ion-implantation process to be a succession of single two-particle collisions. In a recent in-beam Mössbauer experiment<sup>5</sup> on  $^{57}\text{Fe}$  nuclei in aluminum metal, the fraction of implanted Fe ions on interstitial lattice sites was found to be 60%, in good agreement with this collision model.

In this paper we present an extended experimental investigation of ion implantation utilizing the magnetic

hyperfine interaction in a PAD measurement.<sup>6</sup> Fe ions were implanted into the two isomorphous face-centered-cubic phases of Ce metal. The results are compared with predictions of a refined Monte Carlo simulation for the transport of ions in matter (TRIM),<sup>7,8</sup> leading to an excellent agreement in this first application of such a code for the prediction of final lattice site occupancies.

The experiment was performed at the heavy-ion accelerator combination VICKSI. The excited and spin-aligned isomeric  $^{54}\text{Fe}$  nuclei were created in the nuclear reaction  $^{45}\text{Sc}(^{12}\text{C}, 2np)^{54}\text{Fe}$  with a pulsed  $^{12}\text{C}$ -ion beam of 42-MeV kinetic energy hitting the target of a thin Sc foil (1 mg/cm<sup>2</sup>) closely attached to the sample of Ce metal. By their recoil energy of approximately 9 MeV, the Fe ions were implanted (up to a depth of about 5  $\mu\text{m}$ ) into the samples mounted on the cold tip of a temperature-controlled continuous-He-flow cryostat suitable for ion-beam measurements in the high-field superconducting split-pair magnet SULEIMA.<sup>9</sup> The Ce samples (99.999% nominal purity) were prepared in an argon glove box and transferred to the accelerator vacuum by an air lock. The  $\alpha$  phase of cerium was obtained from annealed (700 K for 20 min)  $\gamma$ -Ce by lowering the temperature as well as by application of pressure at 0.8 GPa at room temperature. In the latter case, the pure  $\alpha$ -Ce sample was cooled to 78 K, reduced to normal pressure, and, while held at 78 K, mounted on a precooled cold plate, using an air lock.

Magnetic hyperfine interactions of the nuclear moment ( $g=0.7281$ ) of the isomeric  $I^\pi=10^+$  state ( $\tau=515$  ns), at an excitation energy of 6527 keV in  $^{54}\text{Fe}$ ,<sup>1</sup> were measured in an external magnetic field of  $B_{\text{ext}}=8.15$  T. The field at the site of the nucleus is modified by hyperfine-field contributions  $B_{\text{hf}}$ , when spin or orbital moments are involved. The paramagnetic enhancement factor is defined as  $\beta(T)=B_{\text{eff}}/B_{\text{ext}}$  (Ref. 10) (effective field  $B_{\text{eff}}=B_{\text{ext}}+B_{\text{hf}}$ ). In the case of  $\beta(T)<1$ , the orbital moment of the Fe probes is quenched and only the spin moment is preserved. Here  $\beta(T)\equiv 1$  indicates non-

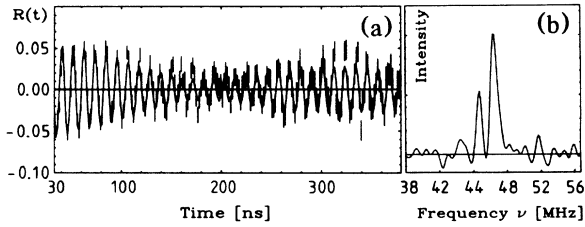


FIG. 1. (a) Spin-rotation pattern of  $^{54}\text{Fe}$  in Ce at  $T=143$  K. (b) Fourier-transformed pattern.

magnetic behavior<sup>11</sup> of the probe ions. Experimentally,  $\beta(T)$  is deduced from the Larmor precession  $\omega_L(T) = \hbar^{-1} g \mu_N B_{\text{eff}}(T)$ , where  $\mu_N$  denotes the nuclear magneton. Thus  $\beta(T) = \omega_L(B_{\text{eff}}(T)) / \omega_L(B_{\text{ext}})$ . The values for  $\omega_L$  were extracted from the spin-rotation-time spectra.<sup>11</sup> In order to allow for two distinct frequencies, i.e.,  $\omega_{L1}$  and  $\omega_{L2}$ , the function

$$R(t) = A_1 G_1 \cos[2(\omega_{L1} - t)] + A_2 G_2 \cos[2(\omega_{L2} - t)] \quad (1)$$

was used to fit the spin-rotation spectra. Here,  $A_i$  denote the amplitudes of the Larmor frequencies  $\omega_{Li}$ , which directly indicate the fractions of implanted ions. The damping functions  $G_i(t) = [0.245 + 0.755] \exp(-\lambda_i^2 t^2 / 0.370)$  are governed by the respective damping parameters  $\lambda_i$ ;<sup>11,12</sup>  $\theta$  denotes the detector angle with respect to the beam direction.

In Fig. 1 an example of a spin-rotation spectrum is shown. The data are fitted with Eq. (1). The fact that two frequencies are involved is revealed by the beat structure found at all measurements below 350 K. At about room temperature the two frequencies differ only by approximately 1%. Their discrimination was achieved by the application of the high external field, which allows a sufficiently precise measurement. Results of all frequency measurements are presented in Fig. 2, where  $\beta$  is plotted as a function of the inverse temperature. Whereas one fraction is nearly temperature independent (nearly constant  $\omega_L$  values), the second one clearly exhibits Curie-like behavior explained by a preserved spin moment. From a linear fit to the data, the two functions

$$\beta_1 = 1.0161(12) - 0.103(75)/T, \text{ nonmagnetic fraction,}$$

$$\beta_2 = 1.0162(42) - 4.08(41)/T, \text{ magnetic fraction,}$$

are obtained and shown as solid lines in Fig. 2. The sum  $A = A_1 + A_2$  of the related amplitudes slightly increases with increasing temperature, as is generally expected due to defect annealing. The analysis of the amplitudes revealed the ratio  $A_1/A_2$  to be constant with temperature over a wide range, indicating that dynamical effects such as diffusion seem to play no role in this temperature region. The nonmagnetic fraction comes out to be the considerably larger one. Of the probe nuclei 75(5)% are nonmagnetic while only 25(5)% show a Curie-like magnetism. At 350 K no discrimination of two frequen-

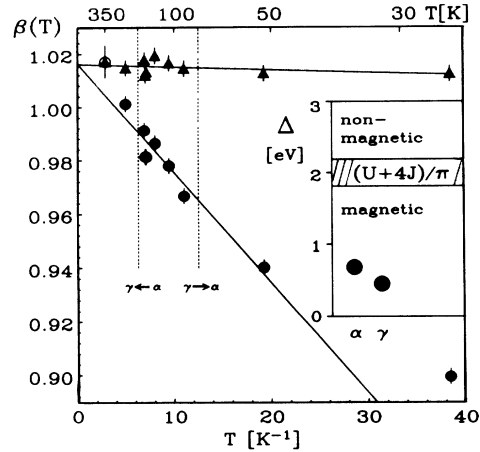


FIG. 2. The paramagnetic enhancement factor  $\beta(T)$  as a function of the inverse temperature. The  $\beta(T)$  values for the two probe fractions show different, magnetic (●) and nonmagnetic (▲), behavior. The vertical dashed lines represent the  $\alpha$ - $\gamma$  phase transitions in cerium. Inset: The values of the hybridization width  $\Delta$  (see text) for substitutional lattice sites in  $\alpha$ - and  $\gamma$ -cerium. The Anderson criterion for the formation of local moments for Fe ions in Ce is indicated by a shadowed bar.

cies was possible. A plot of the relative amplitudes versus temperature is given in Fig. 3. In the present experiment, a small fraction (20%–25%; estimated from comparison of anisotropy amplitudes of  $^{54}\text{Fe}$  probes in different metallic hosts at higher temperatures<sup>13</sup>) of the implanted ions come to rest in disturbed lattice areas, where strong electric-field gradients decrease the nuclear alignment in very short times. Thus, these probe nuclei do not contribute to the measurements at all. Our results are thereby representative for implanted ions located in lattice sites with a well-defined local environment.

We now discuss the conditions for magnetic and nonmagnetic behavior of Fe ions in the fcc lattices of Ce

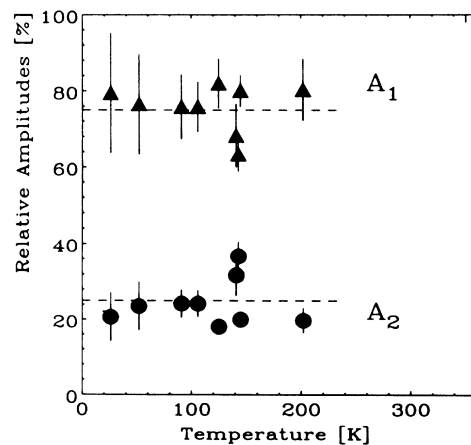


FIG. 3. Relative amplitudes of the spin-rotation spectra as a function of temperature. Dashed lines represent averaged values.

metal. In cerium, the conduction band predominantly contains  $d$ -like electrons. The formation of a local spin moment depends on the balance of the hybridization between the iron  $3d$  electrons with the conduction electrons of the cerium host and the intra-atomic Coulomb ( $U$ ) and exchange ( $J$ ) energies of the  $3d$  electrons. This interaction leads to broadened virtual bound  $d$  states which are characterized by their hybridization width  $\Delta$  (half width at half maximum). According to the Anderson model,<sup>14</sup> conditions favoring the formation of a local spin moment can be quantified by  $\Delta \leq (U+4J)/\pi$ . Using values for  $U$  and  $J$  based on recent spectroscopic data,<sup>15</sup>  $(U+4J)/\pi=2.0(5)$  eV was estimated. A measure of  $\Delta$  may be obtained by the ratio of the volume of the transition-element ion,  $r_{3d}^3$ , and the volume of the Wigner-Seitz cell,  $r_{WS}^3$ . An estimate according to van der Marel and Sawatzky<sup>15</sup> results in  $\Delta = \frac{3}{4} E_F Z [r_{3d}^3 / r_{WS}^3]$ . ( $Z$  and  $E_F$  denote the valence and Fermi energy of the host, respectively.)

For a first approximation we took the uncorrected Wigner-Seitz cell volumes of  $\gamma$ -Ce (20.7 cm<sup>3</sup>/mole) and  $\alpha$ -Ce (15% reduced) for regularly positioned Fe atoms in the Ce host.<sup>16</sup> The Fermi energies for  $\gamma$ -Ce and  $\alpha$ -Ce were taken from Pickett, Freeman, and Koelling.<sup>17</sup> The intra-atomic energy  $(U+4J)/\pi$  in these host metals is compared with the hybridization width  $\Delta$  in the inset in Fig. 2. As is illustrated in Fig. 2, the magnetic behavior of Fe in the two different sites in Ce is not influenced by the phase transition. In the case of the host atom Ce itself, or recoil-implanted Sm,<sup>18</sup> the local magnetic behavior, in fact, relates to the Ce phases. The inset in Fig. 2 in addition gives the explanation of why the considerable volume decrease, when going from the  $\gamma$  to the  $\alpha$  phase of cerium, does not suffice to destroy the magnetic moments of Fe probes at substitutional sites. Although quantitative estimates of the volumes occupied by interstitially positioned Fe atoms are rather difficult, their smaller volumes will certainly result in larger  $\Delta$  values towards the nonmagnetic region (see inset, Fig. 2). We therefore conclude that the magnetic Fe ions replace substitutional Ce ions, while the nonmagnetic fraction is assigned to interstitial sites.

So far we have considered the magnetic behavior in order to identify the lattice positions of the implanted ions. A different approach for the identification of the two fractions is achieved by the application of alloying and implantation models. Miedema and Niessen<sup>3</sup> have used experimental data on the formation of binary alloys in order to predict macroscopic variations in the alloy volume compared to the volumes of the components. These empirical predictions are based on an atomic model, in which volume effects are related to charge transfer.

With the parametrization of Miedema and Niessen, a volume decrease  $\Delta V_m = -2.9$  cm<sup>3</sup>/mole is calculated for Fe in Ce. It reveals that the apparent molar volume of Fe in the cerium host,  $V = V_{Fe} + \Delta V_m = 4.2$  cm<sup>3</sup>/mole, is strongly reduced compared with the molar volume of

pure iron,  $V_{Fe} = 7.1$  cm<sup>3</sup>/mole. The large decrease in volume clearly favors interstitial occupation as Miedema and Niessen have pointed out for comparable cases like Fe in La. Consistency with this alloying model is achieved if we again assign the Fe ions of the larger fraction (75%) with interstitial ones. In order to obtain a quantitative estimate of the interstitial and substitutional lattice site occupations, we now discuss two implantation models.

In a collision model, Brice<sup>4</sup> treats the implantation as a succession of binary collisions. Generally, a host atom is displaced if the energy  $T$  transformed from the incident projectile with kinetic energy  $E$  is larger than the displacement threshold energy  $E_d$  of the host atoms. The scattered projectile is assumed to be captured by the resultant vacancy, if its remaining energy,  $E - T$ , is less than  $E_c$ , the capture threshold energy. Brice's model predicts this probability to depend on  $E_d$ , the kinematic factor  $\gamma = 4M_{\text{host}}M_{\text{probe}}/(M_{\text{host}} - M_{\text{probe}})^2$ , and the parameter  $\rho$ , which is a function of the interaction potential between two collision partners, the impact parameter, and  $E_d$ . Taking  $E_d = 20$  eV,<sup>19</sup> the probability for substitutional lattice positions becomes 34(5)% for  $\gamma$ -Ce and 38(4)% for  $\alpha$ -Ce, in reasonable agreement with the experimental values.

The results of the application of the TRIM (Refs. 7 and 8) program are in remarkably good agreement with the experimental data. In TRIM, the ions or recoils are followed throughout their slowing-down process in three-dimensional motion. The electronic loss during their free flight path between collisions is subtracted before entering the next elastic binary collision. This means that electronic and nuclear energy losses are separated, which is a necessary approach at low energies, where the electronic stopping is due to the conduction electrons and no inner-shell excitation occurs. Here, semiempirical stopping powers<sup>20</sup> are used which are suitable for projectile motions in metals. The implantation process ends in a replacement collision, when the following three conditions are fulfilled simultaneously: (1)  $T > E_b$ , (2)  $E - T < T - E_b$ , and (3)  $E - T < E_{d\text{proj}}$ .  $E_{d\text{proj}}$  denotes the displacement threshold energy of the projectile. It is usually defined as the minimum energy which the projectile needs to move out of the recombination volume of the vacancy.  $E_b$  describes the binding energy of the host atoms in their stable lattice sites, which is usually set equal to the heat of the formation of a vacancy,  $\Delta H_f^{1c} = 1-3$  eV in metals. The above-mentioned conditions reflect the following considerations: Condition (1) is the necessary condition to create a vacancy in the host material (at least temporarily). Condition (2) means that the energy of the projectile after the collision,  $E - T$ , is smaller than the energy of the removed target atom; i.e., the projectile stops sooner and has a higher probability for recombination with the vacancy than the recoiling target atom. The final condition (3) requires that the projectile energy is small enough to ensure that

the projectile does not escape from the recombination volume. With simple kinematic considerations, we obtained a critical energy window of  $5.5 \text{ eV} < E < 176 \text{ eV}$  where replacement collisions may occur, in the case of host and projectile masses of  $M_{\text{host}}=140$  (Ce) and  $M_{\text{probe}}=54$  (Fe) and assuming  $E_b=3 \text{ eV}$  and  $E_{d\text{proj}}=40 \text{ eV}$ . Displacement energies have been measured in the regime of 15 eV (for light elements) to 40 eV (heavy elements), e.g., Ref. 21. In our example, 40 eV was chosen to obtain the largest possible energy window. At higher projectile energies large cascades may be created, but the projectile always escapes the cascade region.

In the Monte Carlo simulations all histories were started well above  $E_{\text{max}}=176 \text{ eV}$  in order to obtain a well distributed slowing-down flux when entering the critical window. With sufficiently high statistics, i.e., using more than  $10^4$  histories, it was found that the replacements are very weakly dependent on  $E_b$  and  $E_d$  as well as on the density of the host material ( $\gamma$ -Ce and  $\alpha$ -Ce), but strongly dependent on the kinematic factor  $\gamma$ . The final result of the computations is that 24(1)% of the Fe ions occupy substitutional lattice positions in Ce metal after implantation.

In conclusion, the present experiment illustrates how the different magnetic responses to an external applied field are used to determine different lattice sites. The majority of Fe ions, when implanted into cerium, come to rest at interstitial lattice sites in agreement with theoretical considerations. The experimental results indicate that 25(5)% of the probe ions replace regularly located host atoms. No influence of the different lattice parameters in  $\gamma$ -Ce and  $\alpha$ -Ce was observed. These findings are also confirmed by the TRIM calculations.

This behavior of Fe in Ce is not unique. For comparison,  $^{54}\text{Fe}$  ions were also implanted into La, Sc, and Bi. In these noncubic hosts as well we observed two-frequency spin-rotation patterns with somewhat different fractions. The measurements of their temperature dependence are not yet completed. Many other PAD experiments on local magnetic moments have been performed, where, however, a lattice-site determination was not considered or a substitutional occupation was assumed (e.g., Ref. 22), or it was not at all clear where the magnetic ions were located.<sup>23</sup> Even two-frequency measurements have been mentioned, without any identification of lattice sites.<sup>24</sup> The present Letter describes the first example where the final site occupation—as an important aspect in any detailed study of the implantation process—is determined.

<sup>1</sup>P. Raghavan, *At. Data Nucl. Data Tables* **42**, 189 (1989).

<sup>2</sup>J. M. Poate and A. G. Cullis, in *Treatise on Materials Science and Technology*, edited by J. K. Hirvonen (Academic, Oxford, 1980), Vol. 18, pp. 85–133.

<sup>3</sup>A. R. Miedema and A. K. Niessen, *Physica (Amsterdam)* **114B**, 367 (1982).

<sup>4</sup>D. K. Brice, in *Application of Ion Beams to Materials—1975*, edited by G. Carter, J. S. Collion, and W. A. Grant, IOP Conference Proceedings No. 28 (Institute of Physics, London, 1976), p. 334.

<sup>5</sup>M. Menningen, R. Sielemann, G. Vogl, Y. Yoshida, K. Bonde-Nielsen, and G. Weyer, *Europhys. Lett.* **3**, 927 (1987).

<sup>6</sup>Part of the data were presented in H. H. Bertschat, K. Biedermann, H. Haas, R. Kowallik, H.-E. Mahnke, W. Müller, S. Seeger, B. Spellmeier, and W.-D. Zeitz, in *Proceedings of the First International Symposium on Swift Heavy Ions in Matter, Caen, France* [Rad. Effects Defects Solids **110**, 105 (1989)].

<sup>7</sup>J. P. Biersack and L. G. Haggmark, *Nucl. Instrum. Methods* **174**, 257 (1980).

<sup>8</sup>J. P. Biersack and W. G. Eckstein, *Appl. Phys. A* **34**, 73 (1984).

<sup>9</sup>P. Jarvis, *J. Phys. (Paris), Colloq.* **45**, C1-803 (1984).

<sup>10</sup>L. Günther and I. Lindgren, in *Perturbed Angular Correlations*, edited by E. Karlsson, E. Matthias, and K. Siegbahn (North-Holland, Amsterdam, 1964), p. 357.

<sup>11</sup>H.-E. Mahnke, *Hyperfine Interact.* **49**, 77 (1989).

<sup>12</sup>E. Dafni and G. D. Sprouse, *Hyperfine Interact.* **4**, 777–781 (1978).

<sup>13</sup>M. H. Rafailovich, E. Dafni, H. E. Mahnke, G. D. Sprouse, and E. Vapirev, *Hyperfine Interact.* **10**, 821 (1981); M. H. Rafailovich, Ph.D. thesis, State University of New York at Stony Brook, 1980 (unpublished).

<sup>14</sup>W. Anderson, *Phys. Rev.* **124**, 41 (1961).

<sup>15</sup>D. van der Marel and G. A. Sawatzky, *Phys. Rev. B* **37**, 10674 (1988).

<sup>16</sup>A. R. Miedema and A. K. Niessen, *CALPHAD: Int. Res. J. Calc. Phase Diagrams* **7**, 51–70 (1983).

<sup>17</sup>W. E. Pickett, A. J. Freeman, and D. D. Koelling, *Phys. Rev. B* **23**, 1266 (1981).

<sup>18</sup>W. Müller, H. H. Bertschat, H. Haas, H.-E. Mahnke, and W.-D. Zeitz, *Phys. Rev. B* **40**, 9346 (1989).

<sup>19</sup>J. N. Daou, E.-B. Hannech, P. Vадja, A. Lucasson, and P. Lucasson, *Philos. Mag. A* **41**, 225–239 (1980).

<sup>20</sup>J. F. Ziegler, J. P. Biersack, and U. Littmark, in *The Stopping and Range of Ions in Solids*, edited by J. F. Ziegler (Pergamon, New York, 1985).

<sup>21</sup>P. Jung, *J. Nucl. Mater.* **117**, 70 (1983).

<sup>22</sup>M. H. Rafailovich, E. Dafni, H.-E. Mahnke, and G. D. Sprouse, *Phys. Rev. Lett.* **50**, 1001 (1983).

<sup>23</sup>D. Riegel, H. J. Barth, L. Büermann, H. Haas, and Ch. Stenzel, *Phys. Rev. Lett.* **57**, 388 (1986); R. Kowallik, H. H. Bertschat, K. Biedermann, H. Haas, W. Müller, B. Spellmeier, and W.-D. Zeitz, *Phys. Rev. Lett.* **63**, 434 (1989).

<sup>24</sup>D. Riegel, L. Büermann, K. D. Gross, M. Luszik-Bhadra, and S. N. Mishra, *Phys. Rev. Lett.* **62**, 316 (1989); S. N. Mishra, K. D. Gross, L. Büermann, M. Luszik-Bhadra, and D. Riegel, *Phys. Rev. Lett.* **63**, 2594 (1989).